

# SECURITY

---

# MARKING

The classified or limited status of this report applies to each page, unless otherwise marked.

Separate page printouts MUST be marked accordingly.

---

THIS DOCUMENT CONTAINS INFORMATION AFFECTING THE NATIONAL DEFENSE OF THE UNITED STATES WITHIN THE MEANING OF THE ESPIONAGE LAWS, TITLE 18, U.S.C., SECTIONS 793 AND 794. THE TRANSMISSION OR THE REVELATION OF ITS CONTENTS IN ANY MANNER TO AN UNAUTHORIZED PERSON IS PROHIBITED BY LAW.

NOTICE: When government or other drawings, specifications or other data are used for any purpose other than in connection with a definitely related government procurement operation, the U. S. Government thereby incurs no responsibility, nor any obligation whatsoever; and the fact that the Government may have formulated, furnished, or in any way supplied the said drawings, specifications, or other data is not to be regarded by implication or otherwise as in any manner licensing the holder or any other person or corporation, or conveying any rights or permission to manufacture, use or sell any patented invention that may in any way be related thereto.

**BEST  
AVAILABLE COPY**



6 May 1965

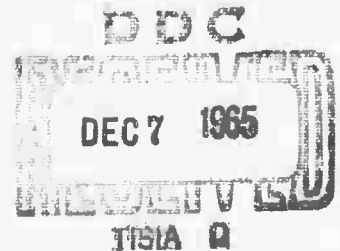
Special Report 1  
Stanford Research Institute Project 5414

CORRECTION TO RANGE OF HEAD ECHO FOR BK

by

John Schlobohm

Monitoring Agency  
U.S. Army Missile Command  
Redstone Arsenal, Alabama



This research was sponsored by the Advanced  
Research Projects Agency as part of Project  
DEFENDER under ARPA Order No. 114.

Copy No.

### CORRECTION TO RANGE OF HEAD ECHO FOR BK19

SRI has been involved in the design and development of the DAZZLE radar and analysis of the data derived therefrom. The radar was designed specifically for study of re-entry phenomena at 55 Mc and 153 Mc. It is located at Central Bore on the missile testing range near Woomera, South Australia. Previous results on the first two firings of the Black Knight in the DAZZLE series, BK19 and BK20, have been reported in Semiannual Technical Report V and Special Report 1 for Contract DA-04-200-ORD-1268.

The data analysis has been hampered by the jitter of the head echo within the range gate from one pulse code group to another. Although it was realized in the design of the radar that the position of the head echo in the range gate would need to be determined from one pulse code group to the next, it had been assumed that the head echo would be much stronger than was actually observed. The smaller signal-to-noise ratio measured is due to the degraded antenna performance (two-way gain down 12 db) at 153 Mc caused by mutual coupling in the antenna feed system. Determination of the head location, therefore, requires further effort than had been anticipated.

In order to obtain the required range resolution for the Project DAZZLE radar, the data are recorded on high-speed film with a fast time base. Each successive pulse return is recorded separated in A-scope format (see Fig. 1) with a 25- $\mu$ sec time base. During re-entry the target range rate is on the order of 5 km/sec, thus an automatic range tracking system is required. The high range-resolution data make use of transmitted pulses 0.25  $\mu$ sec long. This pulse return from the re-entry head, as received in a 10-Mc IF bandwidth, does not provide sufficient signal-to-noise ratio to provide reliable range tracking. The range tracking system therefore operates on a 10- $\mu$ sec pulse return, as received in a 100-kc IF bandwidth. The range tracking stability thus obtained is not as good as desired but is the best that can be achieved with the system sensitivity available. In addition, the wake returns behind the head adversely affect the apparent position of the head as the wake behind the head periodically builds up and collapses.

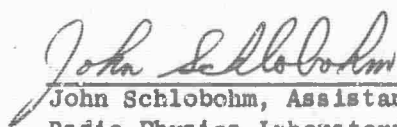
The range tracking unit controls the radar synchronizer which, in turn, determines the timing of the transmitter pulses and corresponding delayed triggers preceding each of the returned echoes. A pulse code is normally transmitted and consists of a tracking pulse 10  $\mu$ sec in length followed 6.1 msec later by a train of pulses termed pulse train A, the first of which is followed 6.1 msec later by another pulse train termed pulse train B. Following the first pulse of train B by 6.1 msec, the tracking pulse and successive pulse trains are again repeated. The pulse width and spacing of pulse trains A and B

are separately controllable, as are the number of pulses within a train up to a maximum of 10. A delayed trigger is generated following each pulse of the pulse code, the amount of the delay being determined by the range tracking system. For a given pulse code consisting of a tracking pulse and two pulse trains, the delay between the transmitted pulse and the delayed trigger is constant to within  $\pm 20$  nsec. The delay is corrected once every pulse train, so that the relative position of the head return with respect to the delayed trigger can change from one pulse train to the next but not within a given train. Correlation studies within a pulse train are therefore readily achievable but are more difficult from one pulse train to the next. Thus, when observing the head echo there is an apparent jitter in range.

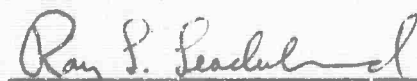
It is possible to measure the relative range from the delayed trigger to the echo return from the second stage, since the second stage produces a strong echo throughout re-entry. This relative delay, as determined by a measurement to the leading edge of the second-stage echo, is plotted in Fig. 2. The relative range between the second stage and the head is known to be a smooth monotonically varying function. In order to obtain a smoothed curve corresponding to the actual position of the second stage, a least-mean-square fit to a third-order polynomial has been made to the points in Fig. 2. The difference between the points and the best-fit trajectory then corresponds to the relative position of the head with respect to the delayed trigger. These values are tabulated in Table I. A negative delay requires that the head echo be shifted closer to the delayed trigger. By shifting each A-scope trace an amount given in Table I, all successive traces should line up so that the position of the head return for successive pulse code groups can be determined.

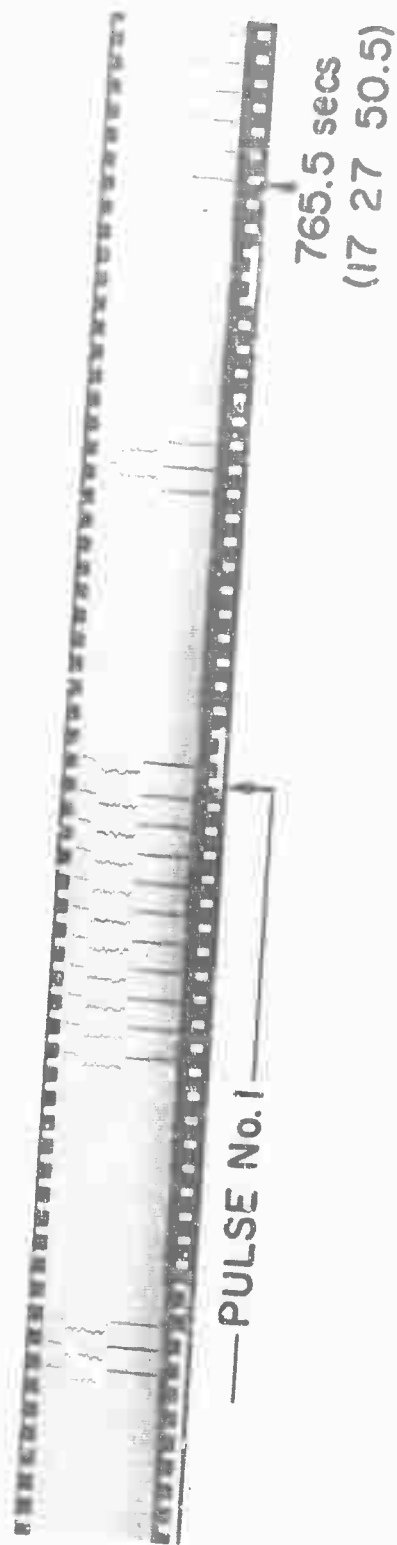
Since the position of the delayed trigger can shift with respect to the head echo from one pulse train to the next, this series of measurements needs to be done for each train separately. The values given in Table I are only for pulse train B, the series of ten pulses spaced 600  $\mu$ sec apart. The measurements presented used the last pulse in each train as indicated by the arrow in Fig. 1. The pulse train corresponding to pulse No. 1 in Table I is defined in Fig. 1. The time shown (time after lift-off and universal time) corresponds to the TIM 100 time marks on the edge of the film.

Submitted by:

  
John Schlobohm, Assistant Manager  
Radio Physics Laboratory

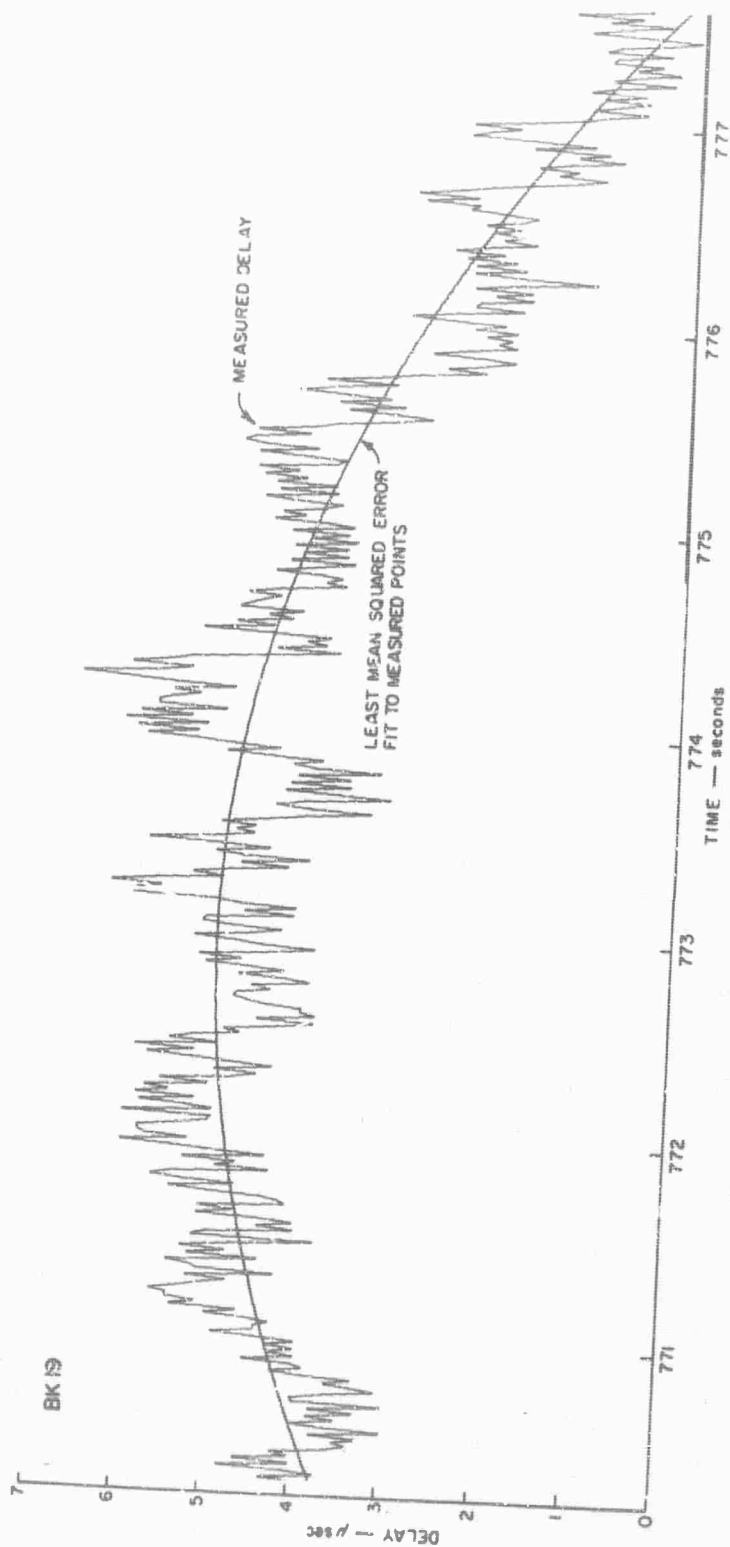
Approved by:

  
Ray L. Leadabrand, Manager  
Radio Physics Laboratory



COMMENCEMENT OF RANGE CORRECTION MEASUREMENT  
FOR BK 19

FIG. 1



DELAY OF SECOND STAGE RETURN RELATIVE TO TRIGGER PULSE AS A FUNCTION OF TIME

FIG. 2

Pulse Code Number	Delay	Pulse Code Number	Delay	Pulse Code Number	Delay
1	-.10 $\mu\text{sec}$	47	-.21 $\mu\text{sec}$	93	-.41 $\mu\text{sec}$
2	-.55 $\mu\text{sec}$	48	-.95 $\mu\text{sec}$	94	-.90 $\mu\text{sec}$
3	.06 $\mu\text{sec}$	49	-.66 $\mu\text{sec}$	95	-.97 $\mu\text{sec}$
4	-.25 $\mu\text{sec}$	50	-.98 $\mu\text{sec}$	96	-.96 $\mu\text{sec}$
5	-.98 $\mu\text{sec}$	51	-.95 $\mu\text{sec}$	97	-.52 $\mu\text{sec}$
6	-.16 $\mu\text{sec}$	52	-1.14 $\mu\text{sec}$	98	-.16 $\mu\text{sec}$
7	-.76 $\mu\text{sec}$	53	-.81 $\mu\text{sec}$	99	-.11 $\mu\text{sec}$
8	-.14 $\mu\text{sec}$	54	-.58 $\mu\text{sec}$	100	-1.12 $\mu\text{sec}$
9	-.31 $\mu\text{sec}$	55	-.25 $\mu\text{sec}$	101	-.09 $\mu\text{sec}$
10	.27 $\mu\text{sec}$	56	-.70 $\mu\text{sec}$	102	-.40 $\mu\text{sec}$
11	.53 $\mu\text{sec}$	57	.29 $\mu\text{sec}$	103	-.91 $\mu\text{sec}$
12	.40 $\mu\text{sec}$	58	-.56 $\mu\text{sec}$	104	-.29 $\mu\text{sec}$
13	.67 $\mu\text{sec}$	59	-.64 $\mu\text{sec}$	105	-.94 $\mu\text{sec}$
14	.18 $\mu\text{sec}$	60	-.88 $\mu\text{sec}$	106	-.57 $\mu\text{sec}$
15	.98 $\mu\text{sec}$	61	.14 $\mu\text{sec}$	107	-.83 $\mu\text{sec}$
16	.36 $\mu\text{sec}$	62	-.63 $\mu\text{sec}$	108	-.12 $\mu\text{sec}$
17	.00 $\mu\text{sec}$	63	-.19 $\mu\text{sec}$	109	-.65 $\mu\text{sec}$
18	.50 $\mu\text{sec}$	64	-.69 $\mu\text{sec}$	110	.14 $\mu\text{sec}$
19	.22 $\mu\text{sec}$	65	-.13 $\mu\text{sec}$	111	.41 $\mu\text{sec}$
20	.74 $\mu\text{sec}$	66	.80 $\mu\text{sec}$	112	-.04 $\mu\text{sec}$
21	.27 $\mu\text{sec}$	67	-.54 $\mu\text{sec}$	113	.60 $\mu\text{sec}$
22	1.08 $\mu\text{sec}$	68	-.36 $\mu\text{sec}$	114	.16 $\mu\text{sec}$
23	.11 $\mu\text{sec}$	69	.60 $\mu\text{sec}$	115	-.29 $\mu\text{sec}$
24	.10 $\mu\text{sec}$	70	.21 $\mu\text{sec}$	116	-.79 $\mu\text{sec}$
25	.49 $\mu\text{sec}$	71	.61 $\mu\text{sec}$	117	-.25 $\mu\text{sec}$
26	1.06 $\mu\text{sec}$	72	.24 $\mu\text{sec}$	118	-.92 $\mu\text{sec}$
27	.79 $\mu\text{sec}$	73	-.43 $\mu\text{sec}$	119	-.00 $\mu\text{sec}$
28	.51 $\mu\text{sec}$	74	-.01 $\mu\text{sec}$	120	-.52 $\mu\text{sec}$
29	.84 $\mu\text{sec}$	75	-.41 $\mu\text{sec}$	121	-.27 $\mu\text{sec}$
30	.31 $\mu\text{sec}$	76	.56 $\mu\text{sec}$	122	.25 $\mu\text{sec}$
31	-.02 $\mu\text{sec}$	77	.48 $\mu\text{sec}$	123	.08 $\mu\text{sec}$
32	.33 $\mu\text{sec}$	78	.30 $\mu\text{sec}$	124	.67 $\mu\text{sec}$
33	.23 $\mu\text{sec}$	79	-.29 $\mu\text{sec}$	125	1.07 $\mu\text{sec}$
34	-.30 $\mu\text{sec}$	80	-.69 $\mu\text{sec}$	126	.44 $\mu\text{sec}$
35	.28 $\mu\text{sec}$	81	.03 $\mu\text{sec}$	127	1.08 $\mu\text{sec}$
36	.00 $\mu\text{sec}$	82	-.55 $\mu\text{sec}$	128	.93 $\mu\text{sec}$
37	.29 $\mu\text{sec}$	83	-.88 $\mu\text{sec}$	129	.94 $\mu\text{sec}$
38	.01 $\mu\text{sec}$	84	-.63 $\mu\text{sec}$	130	.52 $\mu\text{sec}$
39	.33 $\mu\text{sec}$	85	.14 $\mu\text{sec}$	131	.33 $\mu\text{sec}$
40	-.09 $\mu\text{sec}$	86	-.14 $\mu\text{sec}$	132	.18 $\mu\text{sec}$
41	-.57 $\mu\text{sec}$	87	.09 $\mu\text{sec}$	133	.24 $\mu\text{sec}$
42	-.07 $\mu\text{sec}$	88	-.49 $\mu\text{sec}$	134	.60 $\mu\text{sec}$
43	-.06 $\mu\text{sec}$	89	.42 $\mu\text{sec}$	135	.39 $\mu\text{sec}$
44	.10 $\mu\text{sec}$	90	-.16 $\mu\text{sec}$	136	1.04 $\mu\text{sec}$
45	-.14 $\mu\text{sec}$	91	-.61 $\mu\text{sec}$	137	.77 $\mu\text{sec}$
46	-.58 $\mu\text{sec}$	92	-1.18 $\mu\text{sec}$	138	.24 $\mu\text{sec}$



<u>Pulse Code Number</u>	<u>Delay</u>	<u>Pulse Code Number</u>	<u>Delay</u>	<u>Pulse Code Number</u>	<u>Delay</u>
139	.74 $\mu$ sec	185	.78 $\mu$ sec	231	-.81 $\mu$ sec
140	.37 $\mu$ sec	186	1.73 $\mu$ sec	232	-.04 $\mu$ sec
141	-.12 $\mu$ sec	187	1.15 $\mu$ sec	233	-.47 $\mu$ sec
142	.27 $\mu$ sec	188	.55 $\mu$ sec	234	.13 $\mu$ sec
143	-.20 $\mu$ sec	189	1.26 $\mu$ sec	235	-.14 $\mu$ sec
144	.57 $\mu$ sec	190	.59 $\mu$ sec	236	.21 $\mu$ sec
145	1.08 $\mu$ sec	191	1.24 $\mu$ sec	237	-.48 $\mu$ sec
146	.49 $\mu$ sec	192	.66 $\mu$ sec	238	-.38 $\mu$ sec
147	.18 $\mu$ sec	193	1.56 $\mu$ sec	239	-.25 $\mu$ sec
148	-.26 $\mu$ sec	194	.82 $\mu$ sec	240	-.08 $\mu$ sec
149	.35 $\mu$ sec	195	.58 $\mu$ sec	241	-.45 $\mu$ sec
150	.70 $\mu$ sec	196	.89 $\mu$ sec	242	-.12 $\mu$ sec
151	.13 $\mu$ sec	197	.34 $\mu$ sec	243	.58 $\mu$ sec
152	-.17 $\mu$ sec	198	-.17 $\mu$ sec	244	.35 $\mu$ sec
153	-.13 $\mu$ sec	199	.40 $\mu$ sec	245	.70 $\mu$ sec
154	.82 $\mu$ sec	200	-.12 $\mu$ sec	246	.26 $\mu$ sec
155	.27 $\mu$ sec	201	-.53 $\mu$ sec	247	-.25 $\mu$ sec
156	.84 $\mu$ sec	202	-1.10 $\mu$ sec	248	.16 $\mu$ sec
157	.21 $\mu$ sec	203	-.53 $\mu$ sec	249	.59 $\mu$ sec
158	-.03 $\mu$ sec	204	-1.23 $\mu$ sec	250	-.13 $\mu$ sec
159	-1.10 $\mu$ sec	205	-.45 $\mu$ sec	251	.48 $\mu$ sec
160	-1.02 $\mu$ sec	206	-1.39 $\mu$ sec	252	-.02 $\mu$ sec
161	-.66 $\mu$ sec	207	-.64 $\mu$ sec	253	.45 $\mu$ sec
162	-1.23 $\mu$ sec	208	-1.23 $\mu$ sec	254	-.15 $\mu$ sec
163	-.73 $\mu$ sec	209	-.28 $\mu$ sec	255	.51 $\mu$ sec
164	.01 $\mu$ sec	210	-1.05 $\mu$ sec	256	.01 $\mu$ sec
165	-.33 $\mu$ sec	211	-1.06 $\mu$ sec	257	.38 $\mu$ sec
166	.05 $\mu$ sec	212	-.92 $\mu$ sec	258	-.25 $\mu$ sec
167	.71 $\mu$ sec	213	-.62 $\mu$ sec	259	.40 $\mu$ sec
168	.18 $\mu$ sec	214	-.93 $\mu$ sec	260	.09 $\mu$ sec
169	.94 $\mu$ sec	215	-.25 $\mu$ sec	261	-.50 $\mu$ sec
170	.17 $\mu$ sec	216	-.97 $\mu$ sec	262	-.18 $\mu$ sec
171	-.10 $\mu$ sec	217	-1.48 $\mu$ sec	263	-.45 $\mu$ sec
172	.49 $\mu$ sec	218	-2.00 $\mu$ sec	264	-.01 $\mu$ sec
173	-.05 $\mu$ sec	219	-1.11 $\mu$ sec	265	.16 $\mu$ sec
174	-.86 $\mu$ sec	220	-.79 $\mu$ sec	266	-.33 $\mu$ sec
175	-.12 $\mu$ sec	221	-1.48 $\mu$ sec	267	-.71 $\mu$ sec
176	.29 $\mu$ sec	222	-1.08 $\mu$ sec	268	.06 $\mu$ sec
177	.08 $\mu$ sec	223	-.84 $\mu$ sec	269	-.59 $\mu$ sec
178	.29 $\mu$ sec	224	-.02 $\mu$ sec	270	.00 $\mu$ sec
179	-.08 $\mu$ sec	225	.77 $\mu$ sec	271	-.66 $\mu$ sec
180	.44 $\mu$ sec	226	.07 $\mu$ sec	272	-.35 $\mu$ sec
181	.82 $\mu$ sec	227	.59 $\mu$ sec	273	-.84 $\mu$ sec
182	1.54 $\mu$ sec	228	.37 $\mu$ sec	274	-.48 $\mu$ sec
183	.85 $\mu$ sec	229	.61 $\mu$ sec	275	-.95 $\mu$ sec
184	.47 $\mu$ sec	230	-.01 $\mu$ sec	276	-.09 $\mu$ sec

<u>Pulse Code Number</u>	<u>Delay</u>	<u>Pulse Code Number</u>	<u>Delay</u>	<u>Pulse Code Number</u>	<u>Delay</u>
277	-.03 $\mu$ sec	324	.89 $\mu$ sec	371	-.04 $\mu$ sec
278	-.51 $\mu$ sec	325	.22 $\mu$ sec	372	.21 $\mu$ sec
279	-1.02 $\mu$ sec	326	.68 $\mu$ sec	373	.59 $\mu$ sec
280	-.39 $\mu$ sec	327	1.52 $\mu$ sec	374	-.02 $\mu$ sec
281	-.39 $\mu$ sec	328	.68 $\mu$ sec	375	.23 $\mu$ sec
282	-1.24 $\mu$ sec	329	.10 $\mu$ sec	376	.51 $\mu$ sec
283	-1.14 $\mu$ sec	330	.65 $\mu$ sec	377	.01 $\mu$ sec
284	-.56 $\mu$ sec	331	.06 $\mu$ sec	378	.40 $\mu$ sec
285	-1.16 $\mu$ sec	332	.48 $\mu$ sec	379	-.23 $\mu$ sec
286	-.55 $\mu$ sec	333	-.03 $\mu$ sec	380	.00 $\mu$ sec
287	-.32 $\mu$ sec	334	.29 $\mu$ sec	381	.61 $\mu$ sec
288	.27 $\mu$ sec	335	-.27 $\mu$ sec	382	-.10 $\mu$ sec
289	.67 $\mu$ sec	336	.07 $\mu$ sec	383	.10 $\mu$ sec
290	.27 $\mu$ sec	337	.56 $\mu$ sec	384	.57 $\mu$ sec
291	-.29 $\mu$ sec	338	.17 $\mu$ sec	385	.04 $\mu$ sec
292	.29 $\mu$ sec	339	.38 $\mu$ sec	386	.29 $\mu$ sec
293	-.45 $\mu$ sec	340	.02 $\mu$ sec	387	-.29 $\mu$ sec
294	.09 $\mu$ sec	341	.28 $\mu$ sec	388	-.27 $\mu$ sec
295	-.41 $\mu$ sec	342	-.15 $\mu$ sec	389	.27 $\mu$ sec
296	-.95 $\mu$ sec	343	.21 $\mu$ sec	390	-.47 $\mu$ sec
297	-.56 $\mu$ sec	344	.36 $\mu$ sec	391	-.36 $\mu$ sec
298	.07 $\mu$ sec	345	-.02 $\mu$ sec	392	.16 $\mu$ sec
299	-.73 $\mu$ sec	346	-.44 $\mu$ sec	393	.44 $\mu$ sec
300	-.14 $\mu$ sec	347	-.37 $\mu$ sec	394	-.19 $\mu$ sec
301	.25 $\mu$ sec	348	-.99 $\mu$ sec	395	-.82 $\mu$ sec
302	.94 $\mu$ sec	349	-.45 $\mu$ sec	396	-.55 $\mu$ sec
303	.50 $\mu$ sec	350	-1.14 $\mu$ sec	397	.00 $\mu$ sec
304	.80 $\mu$ sec	351	-.70 $\mu$ sec	398	-.75 $\mu$ sec
305	1.20 $\mu$ sec	352	-.40 $\mu$ sec	399	-.43 $\mu$ sec
306	.84 $\mu$ sec	353	.02 $\mu$ sec	400	-1.20 $\mu$ sec
307	.24 $\mu$ sec	354	.48 $\mu$ sec		
308	.59 $\mu$ sec	355	.76 $\mu$ sec		
309	1.11 $\mu$ sec	356	.20 $\mu$ sec		
310	.88 $\mu$ sec	357	.39 $\mu$ sec		
311	1.00 $\mu$ sec	358	-.07 $\mu$ sec		
312	.70 $\mu$ sec	359	.23 $\mu$ sec		
313	1.02 $\mu$ sec	360	.79 $\mu$ sec		
314	.52 $\mu$ sec	361	.26 $\mu$ sec		
315	.83 $\mu$ sec	362	.57 $\mu$ sec		
316	.25 $\mu$ sec	363	-.29 $\mu$ sec		
317	-.26 $\mu$ sec	364	.34 $\mu$ sec		
318	.20 $\mu$ sec	365	-.34 $\mu$ sec		
319	.93 $\mu$ sec	366	-1.08 $\mu$ sec		
320	.36 $\mu$ sec	367	-.89 $\mu$ sec		
321	.40 $\mu$ sec	368	-.61 $\mu$ sec		
322	.95 $\mu$ sec	369	-1.16 $\mu$ sec		
323	.50 $\mu$ sec	370	-.51 $\mu$ sec		